Finite difference solutions for nonlinear water waves using an immersed boundary method

Yan Xu, Harry B. Bingham, Yanlin Shao

Department of Mechanical Engineering, Technical University of Denmark

Section for Fluid Mechanics, Coastal and Maritime Engineering

∗yanxucn@mek.dtu.dk, hbb@mek.dtu.dk, yshao@mek.dtu.dk

1. INTRODUCTION

This work is motivated by two observations related to numerical solutions for nonlinear wave-structure interaction. First, the combination of an Immersed Boundary Method (IBM) for the body-boundary and a σ transform for the free-surface and bottom boundary, as adopted by [1], requires the construction of an artificial C2 continuous free-surface inside the body. While this can be done with some success in 2D, it is likely to be much more problematic in 3D. Secondly, the work of [2] shows quite promising results for the application of an IBM technique for all domain boundaries in the context of the Harmonic Polynomial Cell (HPC) method. Thus, the goal of the present work is to investigate the accuracy and efficiency of a finite difference method solution where all of the fluid domain boundaries are introduced using the IBM. We establish the accuracy and convergence of the method for nonlinear wave propagation on both constant- and variable-depth fluids, demonstrating that the accuracy is comparable to that achieved by the σ transform approach. A preconditioned GMRES iterative solution strategy is also developed and shown to give optimal scaling of the solution effort in 2D.

2. THEORETICAL BACKGROUND

A Cartesian coordinate system is chosen with an origin O, a vertical and upwards z-axis and an x-y plane corresponding to the mean water level. The still water depth $h(\boldsymbol{x}) = h(x, y)$, where $\boldsymbol{x} = [x, y]$ is a horizontal vector. The free surface position is given by $z = \eta(\boldsymbol{x}, t)$. Considering the irrotational flow of an incompressible inviscid fluid, a velocity potential $\phi(\boldsymbol{x}, z, t)$ can be found throughout the fluid domain, and the partial derivatives of ϕ with respect to the three space variables result in the corresponding velocity vector $[\boldsymbol{u}, w] = [u, v, w] = (\nabla\phi, \partial_z\phi)$, where $\nabla = (\partial_x, \partial_y)$.

The governing equation in the fluid domain is the Laplace equation. With all known boundary conditions, the potential value across the fluid domain can be obtained by solving the governing equation. When the boundary value problem is solved in the time domain, the boundary conditions include the potential value on the free surface $\tilde{\phi} = \phi(\boldsymbol{x}, \eta, t)$ and the kinematic bottom boundary condition, as written in equation (1a) and (1c) respectively. At the horizontal truncation boundaries, we will apply either Neumann or periodic conditions, depending on the specific case that we are going to solve.

$$\phi = \tilde{\phi}, \qquad z = \eta \tag{1a}$$

$$\nabla^2\phi + \partial_{zz}\phi = 0, \ -h \leq z < \eta \tag{1b}$$

$$\partial_z\phi + \nabla h \cdot \nabla\phi = 0, \ z = -h \tag{1c}$$

The kinematic and dynamic boundary conditions that govern the free surface evolution can be expressed as:

$$\eta_t = -\nabla\eta \cdot \nabla\tilde{\phi} + \widetilde{w}(1 + \nabla\eta \cdot \nabla\eta) \tag{2a}$$

$$\partial_t\tilde{\phi} = -g\eta - \frac{1}{2}(\nabla\tilde{\phi} \cdot \nabla\tilde{\phi} - \widetilde{w}^2(1 + \nabla\eta \cdot \nabla\eta)) \tag{2b}$$

where g is the gravitational acceleration, and $\widetilde{w} = w(\boldsymbol{x}, \eta, t)$ is the vertical velocity on the free surface.

We will consider a 2D computational domain, as shown in Fig. 1. The free surface and bottom both cut through the computational domain and divide it into two parts. The blue solid points are the intersections between the free surface and vertical grid lines, defined as the free surface points. Following the same principle, a series of bottom points can be found and marked as the black solid points. Based on the boundary points, a series of ghost points can be furtherly determined and marked as red squares. The open blue circles are fluid points and the rest small black crosses are dummy points. When the number of horizontal interpolation points is insufficient, without involving dummy points, additional auxiliary fluid points marked as green circles are introduced to address this problem.
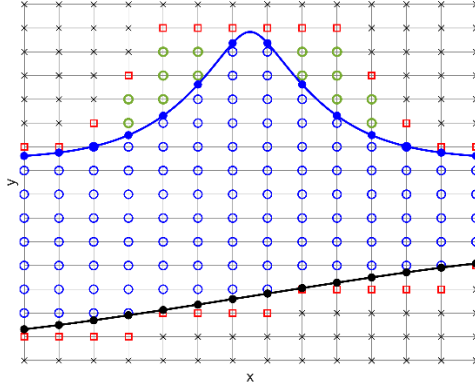
Fig. 1 Finite difference discretization

The dummy points are not involved in any calculations, but in order to maintain a convenient solution logic for the time stepping process, these dummy points are kept in the system, and the potential values are simply set to zero. The potential values on each fluid point are the unknowns, together with the potential values on dummy points, which can be collected into an $N \times 1$ column vector ϕ. The basic idea of the finite difference method to find N finite difference interpolation equations by means of Taylor series expansion and the inversion of a small linear system for all the N unknown values, which can be expressed by an $N \times N$ coefficient matrix $\mathbf{A}$ and an $N \times 1$ vector $\mathbf{d}$ as $\mathbf{A} \phi = \mathbf{d}$.

The robust Generalized Minimal Residual (GMRES) method is employed here to solve this linear system. A linearized second-order version of $\mathbf{A}$ is used as the preconditioning matrix $\mathbf{A_P}$. Due to the constantly changing point distribution in the field, the dummy point information should be first erased from the $\mathbf{A_P}$ prior to each solution.

3. SIMULATION RESULTS

First, the nonlinear traveling wave problem on a flat bottom is solved to verify our approach and quantify its performance. The stream function theory method of [3] is applied to provide initial conditions for η and $\tilde{\phi}$, along with the reference values of $\tilde{w}$ to define the error. Given a wave height H, wave length L, water depth h and a mean Eulerian velocity u_E, a stream function solution can produce the wave elevation η and velocity potential ϕ for a specific wave. It should be noted that the determination of wave height H is related to wave length L and water depth h in the above parameters, by considering the wave breaking limitation given by [4]. We set u_E to zero and apply periodic conditions on the two vertical boundaries.
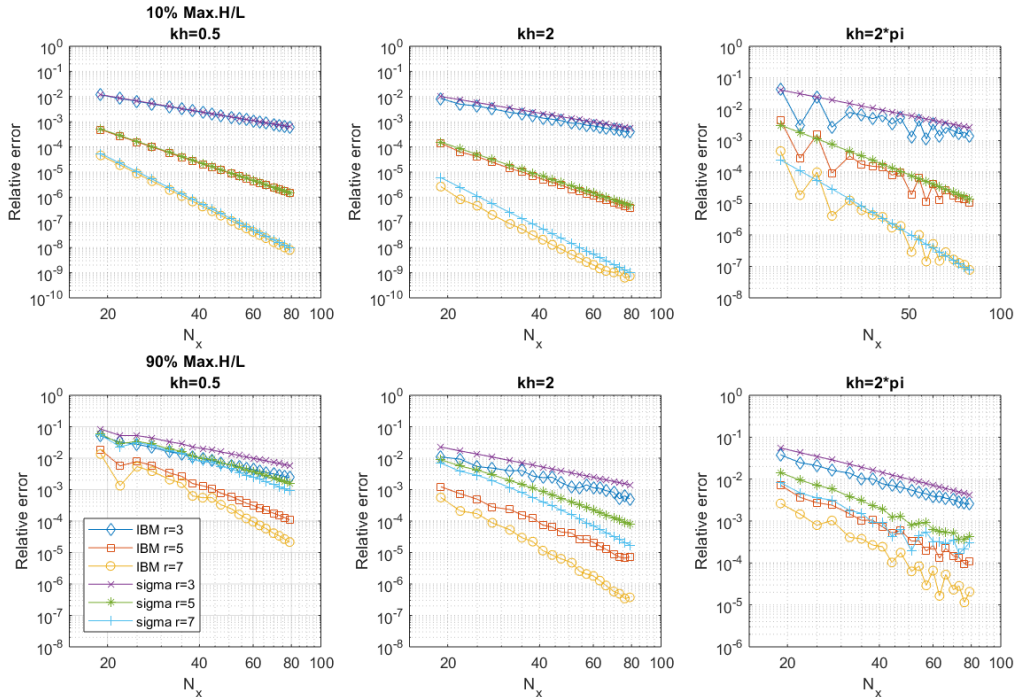
Fig. 2 Nonlinear convergence curves compared to σ transform method

To cover as much as possible of the range of interest, three different relative water depths kh are chosen, representing shallow, intermediate and deep water respectively. For each water depth, both 10% and 90% of maximum steepness cases are considered. The relative error is defined as the 2-norm of the difference between the reference and the computed values of $\tilde{w}$ divided by the 2-norm of the reference value.

Fig. 2 shows the convergence curves for both the IBM and the σ-transform methods. For each curve, the two methods can generally achieve the expected order of convergence before leveling off at an accuracy limit. For the 10% steepness waves, the IBM shows nearly the same level of accuracy as the σ-transform method, except in deep water depth where some oscillations occur in the IBM curves. For the 90% steepness waves, the IBM basically performs better than the σ-transform method, especially in the shallow water cases. This may be explained by the fact that the IBM applies slightly more centered interpolation stencils for the free surface vertical velocity than are applied by the σ-transform method.

As the nonlinearity increases, more iterations are required to achieve convergence for the iterative solution. Fig. 3 shows the average iteration counts for the 90% steepness wave propagating for one wave period, using $N_x = N_z = [19,39,59,79]$. A Courant number of $C_r = 0.35$ has been applied in all cases. The tolerance for the relative residual in GMRES is set to 10^{-7}, and the initial guess is a linear extrapolation from the previous two Runge-Kutta steps. It can be seen that the iteration count is in all cases essentially independent of resolution, and are generally below 15 steps for the second and fourth order schemes, and between 15 and 30 steps for the sixth order scheme.
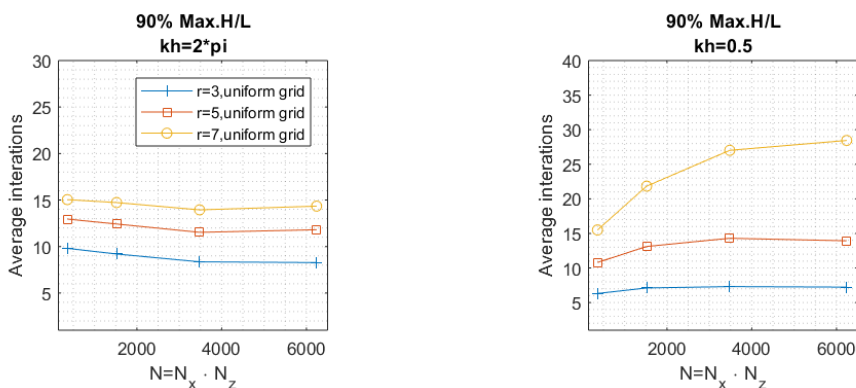
Fig. 3 Average iteration counts for the 90% steepness wave

A nonlinear wave propagation test over a submerged bar is finally conducted to validate the present numerical scheme for solving general nonlinear water wave propagation problems. The nonlinear incident wave is calculated using stream function theory.

The experimental data from [5] is adopted for a comparison. In that experiment, the mean water level is 0.4m, the incident monochromatic nonlinear wave has a 0.02m wave height and wave period of 2.02s. The submerged bar is 0.3m high, the flat top of the bar is 2m long, the up-slope is 0.05 and the down-slope is 0.1. The bar starts at the 6m position after wave generating zone and there is an 8m long flat bottom after the bar. The numerical computational domain follows the experimental bathymetry but adds a wave generation zone and a wave absorption zone at the ends of the domain, both of length two wavelengths. The top plot in Fig. 4 shows the bottom layout and a snapshot of the steady state surface elevation.

The horizontal grid points number $N_x = 674$, the vertical grid points number $N_z = 54$, the Courant number Cr=0.35 at the deep water zone. The grid is clustered around the free surface. A 10th order Savitzky-Golay smoothing filter is applied at each time step to keep the wave propagation stable. A harmonic analysis is performed by making a least-squares fit between the elevation time series and a sum of sinusoids at multiples of the primary wave frequency.

The lower plot of Fig.4 shows the harmonic analysis results. Time series of the elevations at four horizontal positions are shown in Fig. 5. The figures show that the wave steepness first increases dramatically as it shoals up the bar, at the same time the higher order harmonics start to accumulate while the first order wave starts decline after it reaches the top of bar. Then the wave continues propagating through the down-slope and back to the flat bottom, where higher harmonics are released and an irregular wave pattern after the bar is formed. Both the plots indicate a good agreement between the numerical and measured results.

4. CONCLUSION

The accuracy of a finite difference based solution to the exact potential-flow problem for nonlinear waves with an IBM treatment of both the free surface and bottom boundaries has been established in 2D. The IBM is found to be of comparable accuracy to the more commonly used σ-transform method. The IBM approach is expected to be more easily extended to wave-structure interaction problems, which is the next step. Preliminary results have also been presented towards an optimal iterative solution strategy for this method, and this is also a topic of further study.
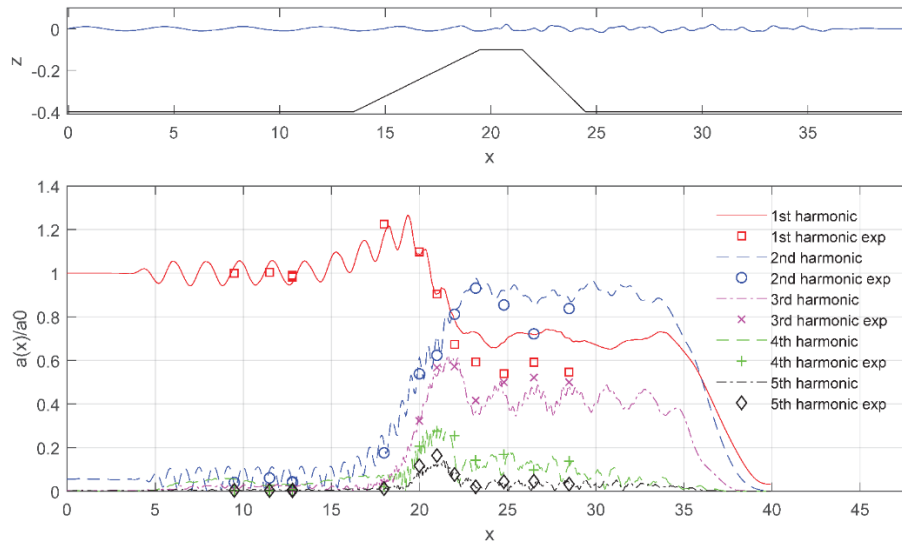
Fig 4. Top: submerged bar geometry layout and the wave surface snapshot.

Bottom: harmonic analysis of the wave elevation time series.
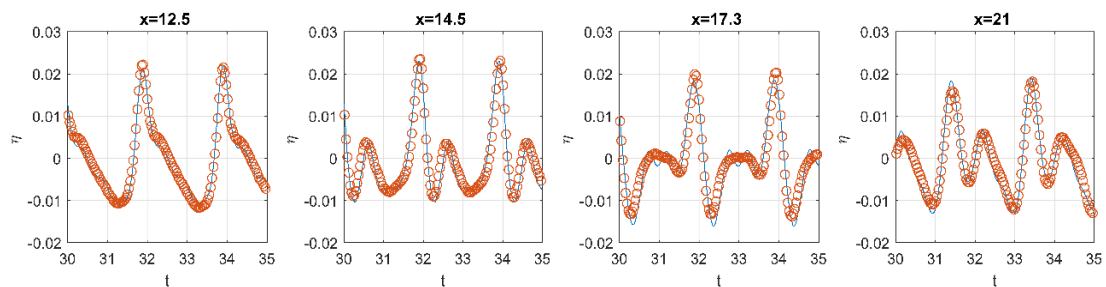
Fig. 5 Time series of wave elevations over the bar. Solid lines – Calculations; Circles – Measurement.

ACKNOWLEDGEMENT

REFERENCES

[1] Kontos, S. *Robust Numerical Methods for Nonlinear Wave-Structure Interaction in a Moving Frame of Reference*. PhD Thesis, Technical University of Denmark. 2016.

[2] Hanssen, F.-C.W., Bardazzi, A., Lugni, C., Greco, M. Free-surface tracking in 2D with the harmonic polynomial cell method: Two alternative strategies. *International Journal for Numerical Methods in Engineering*, **113(2)**: 311-351. 2018.

[3] Fenton, J.D. The numerical solution of steady water wave problems. *Computers & Geosciences*, **14(3)**: 357-368. 1988.

[4] Fenton J.D. Nonlinear wave theories. *The Sea – Vol. 9: Ocean Engineering Science, Part A*, B. Le Méhauté and D.M. Hanes, eds. 1990.

[5] Beji, S., Battjes, J. A. Experimental investigation of wave propagation over a bar. *Coastal Engineering*, **19(1-2)**: 151-162. 1993.